23rd ABCM International Congress of Mechanical Engineering
December 6-11, 2015, Rio de Janeiro, RJ, Brazil

ON THE ROBUST CONTROL OF NONLINEAR AEROELASTIC RESPONSE OF AN AIRFOIL

Natália C. G. de Paula
Daniel A. Pereira
Flávio D. Marques
Engineering School of São Carlos – University of São Paulo
natalia.paula@usp.br, daniel.almeida.pereira@usp.br, fmarques@sc.usp.br

Abstract. *This work is related to the control of aeroelastic response in typical section where nonlinear structural effects are present. This investigation admits the development of numerical and experimental approaches to exam active control laws alternatives in aeroelastic applications. Typical section model in pitching and plunging displacements is considered, where a hardening nonlinear effect in pitch stiffness is included to the problem. Such effect leads the system to typical nonlinear responses and flutter connected to limit cycle oscillations. Control laws are considered admitting first the concept of eigenstructure assignment and robust linear optimal designs, followed by applying fuzzy logic control as a nonlinear approach. Control systems are, then, computationally simulated using experimental apparatus parameters to check on their features and efficiency on controlling nonlinear aeroelastic responses and suppressing flutter phenomenon. As a source of actuation to the active control problem, piezoelectric patches are used. The control authority of this kind of actuation method will also be examined in this investigation.*

Keywords: *Aeroelasticity, optimal control, piezoelectric, active aeroelastic control, structural nonlinearity*

1. INTRODUCTION

Aeroelasticity concerns the field of study which comprises the interaction between elastic deformations of a structure under the force effect of non-stationary aerodynamic flow (Bisphinghoff *et al.*, 1996). The combination of these loads causes, in general, undesirable effects which lead to aircraft performance loss or even failure of the structure. These effects are associated with both static and dynamic phenomena such as divergence, control reversal, buffeting and flutter.

Such problems have become more prominent with arising new technologies, as highly flexible or composite material wings. It is known that these structures are subjected to nonlinear phenomena that might be difficult to predict. Nonlinear behavior origins are both in structural dynamics and in unsteady aerodynamic loads. Different types of structural and aerodynamic nonlinearities are commonly encountered in aeronautical engineering, in this case a comprehensive study of some different types of nonlinearities present on aeroelastic systems and their effects can be found in (Lee *et al.*, 1999). Nonlinear systems may be subject to behaviors such as bifurcations, limit cycle oscillations (LCO), and chaos (Sheta *et al.*, 2002). For example, limit cycle oscillations have caused persistent problems in aircraft designs such as in the F-16, which presents hardening nonlinearity in the connection of external accessories (Chen *et al.*, 1998). There are several other flight experiences with LCOs in addition to the F-16, including those of the F-18, the B-1, and the B-2 (Hartwich *et al.*, 2001; Dobbs *et al.*, 1985; Denegri and Johnson, 2001). Most of these LCOs have been attributed to nonlinear aerodynamic effects due to shock wave motion and/or separated flow (Dowell *et al.*, 2003).

Thus, it is necessary to understand these effects and develop alternatives to eliminate or mitigate them. Several authors have developed control strategies to suppress long term damages associated with nonlinear aeroelastic behavior (Block and Strganac, 1998; Singh and Yim, 2003; Ko *et al.*, 1999). Active solutions may be advantageous and flexible, with the possibility of varying the control law to adapt the system to different operating conditions.

An example of these solutions are smart structures, that incorporate sensors and actuators coupled through a controller. Among smart materials, piezoelectric highlight for vibration control once they can operate on a broad frequency band (Preumont, 2012). Piezoelectric as aeroelastic control device have applications in two different ways: (i) replacing conventional actuators; (ii) as bending motors for vibration suppression. In the first case, the piezoelectric material actuates a control surface to modify the aerodynamic flow and cancel the source of vibrations (Ehlers and Weisshaar, 1993). In the second case, piezoelectric material is part of the structure itself and has a bending response locally transmitted to the structure when electrically stimulated (Robert *et al.*, 1997).

Robust controllers are an alternative to plants whose dynamics contain bounded uncertainties, as for nonlinear aeroelastic systems. The design of this type of controller is oriented to work satisfactory for a set of plants, linear or nonlinear, assuming the operation under the worst-case condition assumption (Lavretsky and Wise, 2013). Linear quadratic regulators and controllers based on H_∞ norm might satisfy these requirements.

This paper presents the study of nonlinear aeroelastic response behavior of an airfoil and the suppression of undesired aeroelastic vibrations to extend LCO and flutter boundaries using piezoelectric actuation. The nonlinear structural behavior is obtained assuming nonlinear hardening moment in pitching represented by a cubic polynomial. An aeroelastic model is accomplished using unsteady aerodynamics formulation of Theodorsen (1935) and experimental data. Three different control strategies are used as a preliminary tool in order to test the control actuation concept for the nonlinear aeroelastic model: (i) eigenstructure assignment, (ii) linear quadratic regulator (LQR), and (iii) fuzzy logic controller. These controllers are designed for the linear system and have the gains applied in the nonlinear condition. An exception is made for the fuzzy controller, which control response decision is invariant to system parameter fluctuations.

2. METHODOLOGY

2.1 Aeroelastic Model

The mathematical model for a typical section with two degrees of freedom and semi-chord b (*cf.* Fig. 1) is derived in Bisphinghoff *et al.* (1996); Fung (1993), that is,

$$\begin{bmatrix} \mu_e & x_\alpha \\ x_\alpha & {r_\alpha}^2 \end{bmatrix} \begin{Bmatrix} \ddot{\xi} \\ \ddot{\alpha} \end{Bmatrix} + \begin{bmatrix} d_{1,1} & d_{1,2} \\ d_{2,1} & d_{2,2} \end{bmatrix} \begin{Bmatrix} \dot{\xi} \\ \dot{\alpha} \end{Bmatrix} + \begin{bmatrix} {\omega_h}^2 & 0 \\ 0 & {r_\alpha}^2 {\omega_\alpha}^2 \frac{F(\alpha)}{\alpha(t)} \end{bmatrix} \begin{Bmatrix} \xi \\ \alpha \end{Bmatrix} = \begin{Bmatrix} -L(t)/m_W b \\ M_\alpha(t)/m_W b^2 \end{Bmatrix} , \quad (1)$$

where the plunge and pitch displacements are given by h and α, respectively, a is the dimensionless distances from the elastic axis to the mid chord, U is the airspeed, x_α is the dimensionless distances from elastic axis to wing center of gravity (CG), r_α is the dimensionless rotational inertia term about elastic axis (EA), k_h and k_α are the plunge and pitch stiffness, respectively, $\xi(t) = \frac{h(t)}{b}$, $\mu_e = \frac{m_T}{m_W}$, m_T and m_W are the total and wing mass, respectively, $d_{i,j}$ are the damping factors with respect to each airfoil motion and their influences (Rayleigh's approach), $L(t)$ is the lift force, M_α is the aerodynamic pitch moment and $F(\alpha)$ is the function related to the nonlinear pitch stiffness.

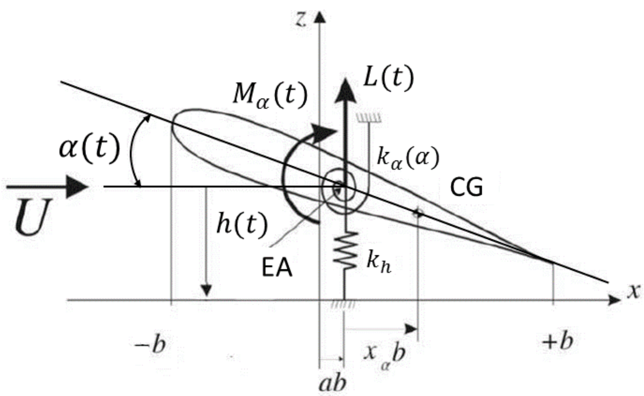

Figure 1: Typical aeroelastic section.

Aerodynamics modeling is based on the formulation by Theodorsen (1935) that presents an analytical solution to the pressure distribution around a typical airfoil section using 2-D irrotational, incompressible and potential flow and written respectively as

$$L(t) = L^{NC} + L^{C} , \quad (2)$$

$$M_\alpha(t) = M_\alpha^{NC} + M_\alpha^{C} , \quad (3)$$

where the non-circulatory terms (superscripts NC) are

$$L^{NC} = \pi \rho b^2 \left[\ddot{h} + U\dot{\alpha} - ba\ddot{\alpha} \right] , \quad (4)$$

$$M_\alpha^{NC} = \pi \rho b^2 \left[ba\ddot{h} - Ub\left(\frac{1}{2} - a\right)\dot{\alpha} - b^2\left(\frac{1}{8} + a^2\right)\ddot{\alpha} \right] , \quad (5)$$

and the circulatory terms (superscripts C) are

$$L^{C} = 2\pi\rho U b C(k) f(t) , \quad (6)$$

$$M_\alpha^C = 2\pi\rho b^2(a + \frac{1}{2})C(k)f(t) \ , \tag{7}$$

where $C(k)$ is the so-called Theodorsen function and

$$f(t) = U\alpha + \dot{h} + \dot{\alpha}b\left(\frac{1}{2} - a\right) \ , \tag{8}$$

is the quasi-steady term (Theodorsen, 1935).

The aerodynamic loading, as given from Eqs. (2) to (3), depends on the Theodorsen function $C(k)$, where $k = \frac{\omega b}{U}$ is the reduced frequency of harmonic oscillations. However, to account for arbitrary motions an alternative is to manipulate the Theodorsen function by convolution based on Duhamel formulation in the time domain (Li *et al.*, 2010). If the Wagner function is also considered, it implies that, for instance, circulatory lift term can be written as

$$C(k)f(t) = f(0)\phi(\tau) + \int_0^\tau \frac{\partial f(\sigma)}{\partial\sigma}\phi(\tau - \sigma)d\sigma \ , \tag{9}$$

where σ is a dummy integration variable, $\tau = \frac{tU}{b}$ is the non-dimensional time and $\phi(\tau)$ is the Wagner function, which using the Sear's approach (Sears, 1940) can be written as

$$\phi(\tau) \approx c_0 - c_1 e^{-c_2\tau} - c_3 e^{-c_4\tau} \ , \tag{10}$$

where $c_0 = 1.0$, $c_1 = 0.165$, $c_2 = 0.0455$, $c_3 = 0.335$ and $c_4 = 0.3$.

Using integration by parts and following the state-space method proposed by Lee *et al.* (1997) and Li *et al.* (2010), Eq. (9) leads to a circulatory term as

$$C(k)f(t) = (c_0 - c_1 - c_3)f(t) + c_2c_4(c_1 + c_3)\overline{x} + (c_1c_2 + c_3c_4)\dot{\overline{x}} \ , \tag{11}$$

where $\overline{x}$ and $\dot{\overline{x}}$ are augmented aerodynamic states.

Substituting Eq. (11) in Eqs. (6) and (7), one can obtain the circulatory aerodynamic loads for the two degrees-of-freedom.

The aeroelastic equations of motion (Eq. (1)) can then be represented in state-space form:

$$\dot{\mathbf{x}} = \mathbf{A}(\mathbf{x})\mathbf{x} \ , \tag{12}$$

where the state vector is $\mathbf{x} = \left[\ \xi(t) \quad \alpha(t) \quad \dot{\xi}(t) \quad \dot{\alpha}(t) \quad \overline{x} \quad \dot{\overline{x}}\ \right]^T$ and the state matrix is

$$\mathbf{A} = \left[\begin{array}{ccc} \mathbf{0_{2\times2}} & \mathbf{I_{2\times2}} & \mathbf{0_{2\times2}} \\ -\mathbf{M_t^{-1}K_t} & -\mathbf{M_t^{-1}B_t} & \mathbf{M_t^{-1}D} \\ \mathbf{E_1} & \mathbf{E_2} & \mathbf{F} \end{array}\right] \ , \tag{13}$$

with $\mathbf{M_t}$, $\mathbf{K_t}$, $\mathbf{B_t}$ being the total mass, stiffness and damping matrices, respectively, including both structural and aerodynamic contributions; $\mathbf{D}$, $\mathbf{E_1}$, $\mathbf{E_2}$ and $\mathbf{F}$ are related to the inclusion of the lag states due to non-stationary aerodynamics.

A detailed description of the terms that compose the matrices in Eq. (13) can be found in Vasconcellos (2012).

Function $F(\alpha)$ in Eq. (1) is used in the aeroelastic equations with the respective terms to account for nonlinearity in pitching response. Figure 2 shows the structural nonlinearity, which is represented by the hardening effect.

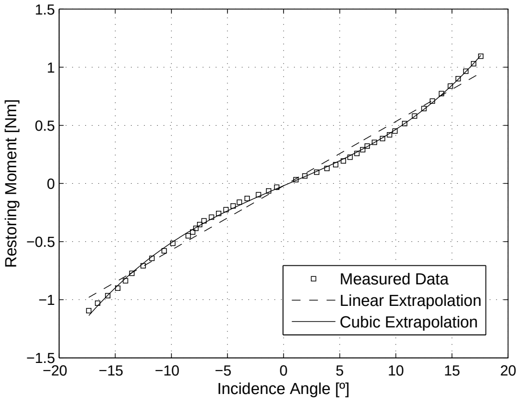

Figure 2: Restoring pitch moment.

Table 1: Polynomial coefficients for nonlinear pitch stiffness approximation (*cf.* Eq. (14)).

COEFF.	VALUES
a_1^1	1.81
a_0^1	0.21
a_3^2	4.25
a_1^2	0.72
a_1^3	1.81
a_0^3	-0.21

Pitch stiffness nonlinearity is defined by a partitioned function. For smaller pitch angles stiffness hardening is represent by a symmetric cubic polynomial. The linear approximation for higher and lower α values constrains LCO to a range of speeds, what better represents the experimental behavior. The non-dimensional coefficients are given in Tab. 1. Measurement data was available only for hardening region and is illustrated in Fig. 2.

$$F(\alpha) = \begin{cases} a_1^1\alpha + a_0^1 & \text{if } \alpha < -\alpha_0 \\ a_3^2\alpha^3 + a_1^2\alpha & \text{if } -\alpha_0 < \alpha < \alpha_0 \\ a_1^3\alpha + a_0^3 & \text{if } \alpha < \alpha_0 \end{cases} \tag{14}$$

where α_0 is chosen to be $0.25rad$

The aeroelastic system is numerically integrated using Runge-Kutta method. Table 2 presents the values under consideration in this work which are based on experimental tests.

Table 2: Experimental values used for the numerical model.

VARIABLES	DESCRIPTION	VALUES
b	Mid-chord (m)	0.125
a	Distance from semichord to elastic axis (nondimensional)	-0.5
ρ	Air density (kg/m^3)	1.087
m_W	Wing mass (kg)	1.5
m_T	Total mass (kg)	3.67
ω_h	Decoupled plunge natural frequency (rad/s)	29.9
ω_α	Decoupled pitch natural frequency (rad/s)	16.27
x_α	Nondimensional distance between elastic axis and CG of wing	0.66
r_α	Nondimensional rotational inertia term about elastic axis	0.73
μ	Nondimensional mass ratio	28.12
$d_{i,j}$	Damping matrix using Rayleigh's approach	$\begin{bmatrix} 0.87 & 0.36 \\ 0.36 & 4.98 \end{bmatrix}$
U_f	Linear flutter velocity (Numeric corrected velocity) (m/s)	13.35

2.2 Piezoelectric Model

An experimental apparatus developed by Vasconcellos (2012) is taken into account to provide modelling parameters for the aeroelastic equations. It consists of a rigid wing suspended by an elastic mounting system with pure pitch and plunge motions (Fig. 3). Pitch mechanism is a single spring steel wire connected to wing's pivot and to a base free to move in plunge degree of freedom. Plunge mechanism consists of four spring steel plates clamped at each end to the apparatus external fixed structure and the moving base. *Midé QuickPack – QP20W* piezoelectric patches will be placed at the root of each spring steel plate to provide enough control authority and to maintain the symmetry of the model. Such topology is modelled as actuation source for the design of the control laws.

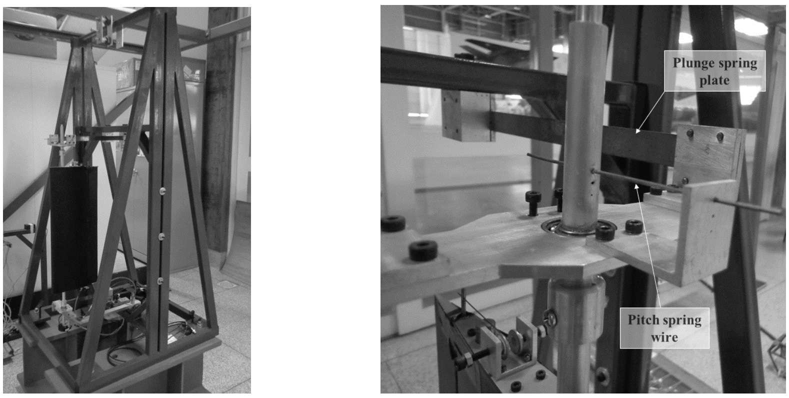

(a) (b)

Figure 3: (a) Overview of experimental apparatus (b) Detail of the elastic mounting.

Piezoelectric patches modelled as rectangular piezoelectric layer has loading effect equivalent to a pair of bending moments M_p applied to its ends (Preumont, 2012). The bearing moment results,

$$M_p = -E_p d_{31} V b z_m \ , \tag{15}$$

in which E_p, d_{31} and b corresponds to piezoelectric Young's modulus, strain constant in in-plane expansion and width, respectively, V is the applied voltage on electrodes and z_m is the distance between the piezoelectric mean line and the beam neutral line.

Plunge stiffness (k_h) is obtained from a finite element analysis of the steel springs using Euler-Bernoulli beam with wide cross-section hypothesis. The boundary conditions that better represent the real system are a clamping at one end and guides at another. For no applied voltage, the error compared to experimental measurements is less than 5%. Applying voltage, beam loading is modified by piezoelectric actuation. Spring restoring force F is no longer dependent only of plunge displacement but also of applied voltage V, that is,

$$F = k_h h + k_V V \ , \tag{16}$$

where k_V is the voltage stiffness constant.

An approximation to map the effect given in Eq. (16) is depicted in (Fig. 4).

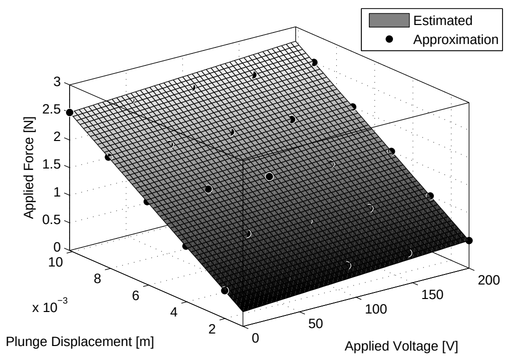

Figure 4: Spring restoring force correlation with applied voltage.

Final state-space equation with piezoelectric control forces included as an input, similarly to Heeg (1993), is

$$\dot{\mathbf{x}} = \mathbf{A}(\mathbf{x})\mathbf{x} + \mathbf{B}u \ , \tag{17}$$

where u is the applied voltage input and the input matrix is

$$\mathbf{B} = \begin{bmatrix} \mathbf{0_{2\times1}} \\ \mathbf{M_t^{-1}} \times \begin{bmatrix} 4k_V/m_W b \\ 0 \end{bmatrix} \\ \mathbf{0_{2\times1}} \end{bmatrix} \ . \tag{18}$$

2.3 Control Laws

It is admitted that all controllers should use an output feedback strategy instead of the design of an state observer to estimate the non-measurable aerodynamic states. Limitations of output feedback in eigenstructure assignment are well presented in Andry *et al.* (1983). The control input is

$$u = -\mathbf{K}\mathbf{y} \ , \tag{19}$$

with $\mathbf{y} = \begin{bmatrix} \xi(t) & \alpha(t) & \dot{\xi}(t) & \dot{\alpha}(t) \end{bmatrix}^T$.

A first strategy to determine the feedback gain matrix $\mathbf{K}$ was the eigenstructure assignment. It followed the steps described in Stevens and Lewis (1992) for the desirable closed loop poles and eigenvectors chosen accordingly to the natural frequencies and damping ratio of a more stable similar system (Block and Strganac, 1998).

The linear quadratic regulator (LQR) is a control methodology that is concerned to the relative importance of the states error and control usage through its optimal approach. Here, the implementation of the LQR with output feedback follows Stevens and Lewis (1992). Discussions on the stability robustness of LQR solutions are presented in Lavretsky and Wise (2013). The LQR approach is based on finding $\mathbf{K}$ that minimizes the performance index, that is,

$$\mathbf{J} = \frac{1}{2}\int_0^\infty (\mathbf{x}^T\mathbf{Q}\mathbf{x} + \mathbf{u}^T\mathbf{R}\mathbf{u})dt \ , \tag{20}$$

with the weighting matrices $\mathbf{Q}$ and $\mathbf{R}$ chosen as

$$\mathbf{Q} = \begin{bmatrix} 1/\alpha_{max}^2 & 0 & 0 & 0 \\ 0 & 1/\xi_{max}^2 & 0 & 0 \\ 0 & 0 & 1/\dot{\alpha}_{max}^2 & 0 \\ 0 & 0 & 0 & 1/\dot{\xi}_{max}^2 \end{bmatrix} \ , \tag{21}$$

where the maximum values were obtained from the controlled response with the eigenstructure assignment strategy and

$$\mathbf{R} = \frac{1}{u_{max}} \ , \tag{22}$$

in which the value of u_{max} is the maximum applicable voltage to the piezoelectric patch of $200V$.

For both previous control methodologies, that is, eigenstructure assignment and LQR, the gain matrices were derived for the linear aeroelastic system at an airspeed 10% above the flutter boundary and fixed to all simulated velocities even in detriment of controller performance.

A fuzzy logic controller is also considered and based on the Mamdani-type fuzzy model. Membership functions are defined from experimentation of the nonlinear aeroelastic model. The set of rules to guide the control action in Tab. 3 is equivalent a PD-type controller as presented by Yager and Filev (1994). The magnitude (Z - zero, S - small, M - medium or L - large), sign (negative or positive) and correlation between input and output signals are represented by the rule basis. The decision surface obtained (Fig. 5) represents the control law on a unitary discourse universe.

Table 3: Rule basis.

		Variation of error						
		-L	-M	-L	Z	+S	+M	+L
Error	-L	-L	-L	-L	-L	-M	-S	Z
	-M	-L	-L	-M	-M	-S	Z	+S
	-S	-L	-M	-S	-S	Z	+S	+M
	Z	-L	-M	-S	Z	+S	+M	+L
	+S	-M	-S	Z	+S	+S	+M	+L
	+M	-S	Z	+S	+M	+M	+L	+L
	+L	Z	+S	+M	+L	+L	+L	+L

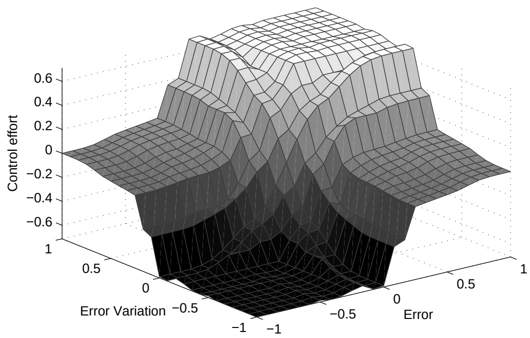

Figure 5: Fuzzy controller decision surface.

The error and the variation of this error defined as control inputs (normalized by individual gains) obeys

$$e(t) = W_{\alpha}\alpha(t) + W_{\xi}\xi(t) \ , \tag{23}$$

$$\Delta e(t) = W_{\dot{\alpha}}\dot{\alpha}(t) + W_{\dot{\xi}}\dot{\xi}(t) \ , \tag{24}$$

where the importance of torsion and bending errors and their variation are quantified by the weights W_{α}, W_{ξ}, $W_{\dot{\alpha}}$ and $W_{\dot{\xi}}$, tuned accordingly to Jantzen (1999) to guarantee a stable system.

3. RESULTS

Figure 6 is representative of how the system behavior is modified by a pitch stiffness hardening. Limit cycle oscillations can be clearly identified for the nonlinear curves. The velocity is $U_{\infty} = 13.8m/s$.

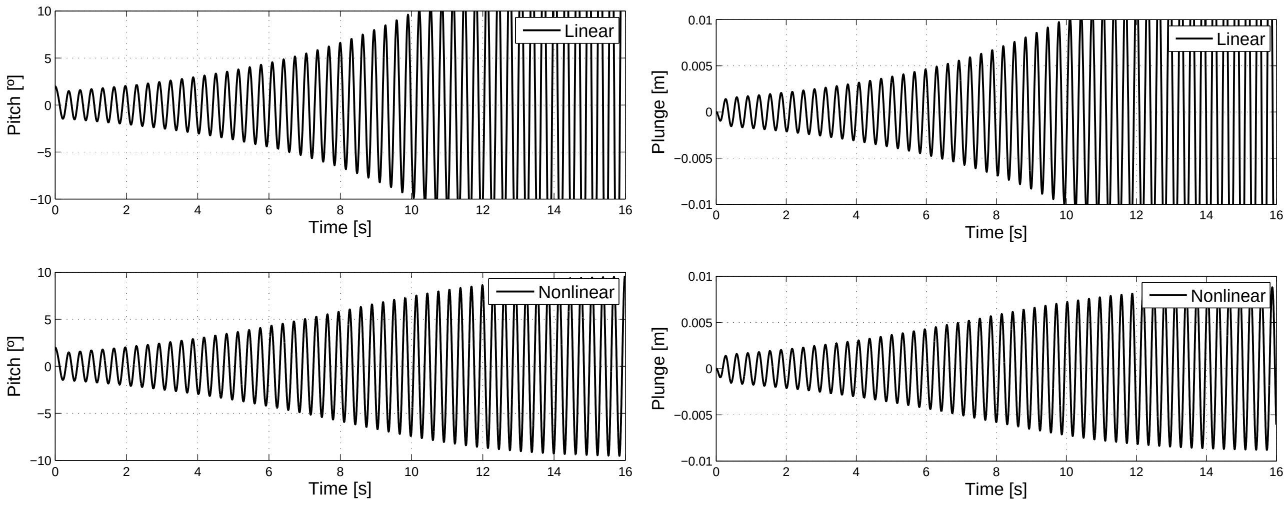

Figure 6: Comparison of pitch and plunge displacements for linear and nonlinear systems at a velocity $U_{\infty} = 13.8m/s$.

The response of the linear and nonlinear systems are given in Fig. 9 for a $0.002m$ plunge initial condition. Both open and closed loop displacements are shown with control activated at the beginning of the simulation for a freestream velocity $U_\infty = 13.8m/s$, a little above the linear flutter speed ($U_{flutter} = 13.35m/s$).

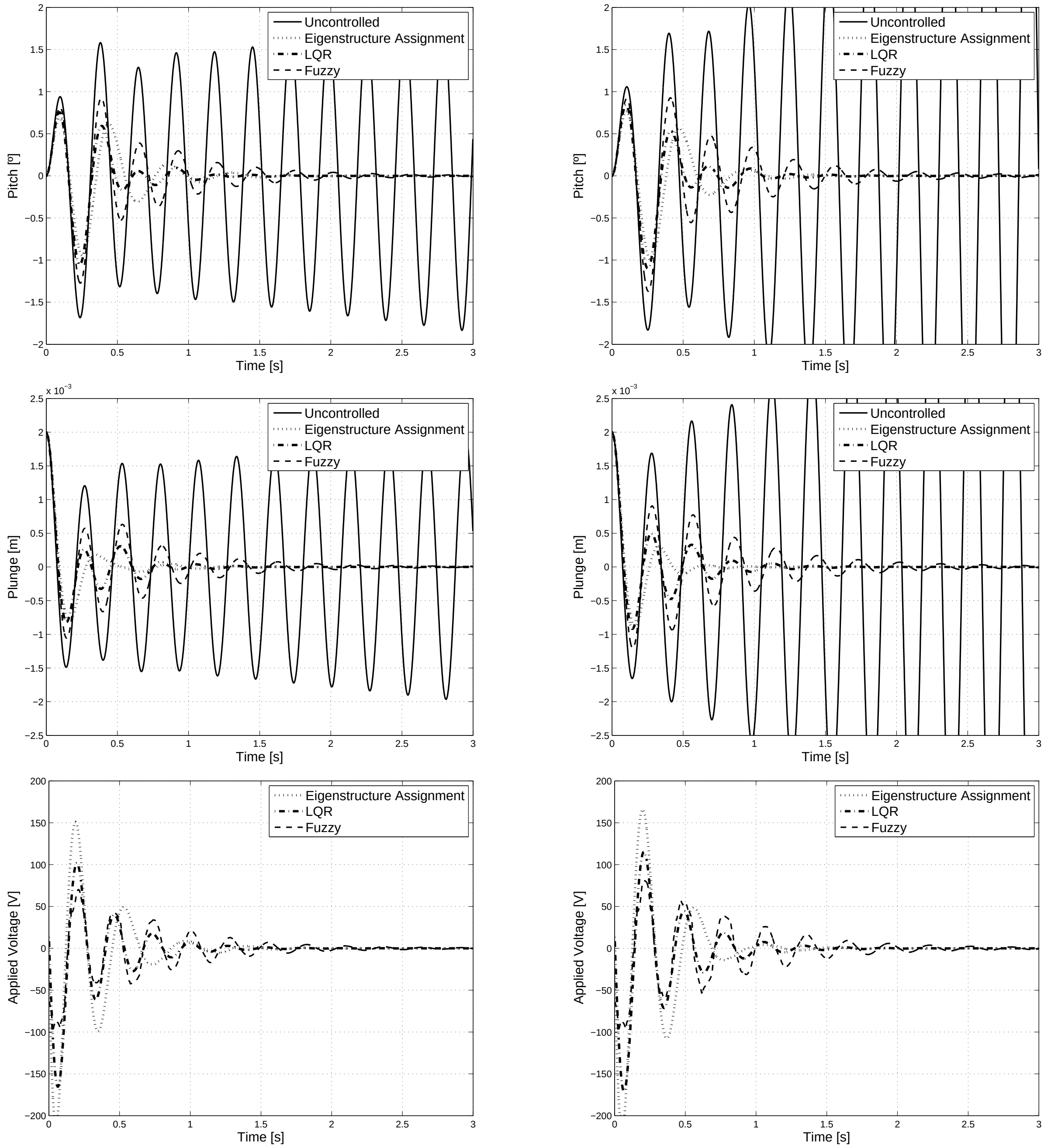

Figure 9: Response of the linear system in the left-side view for $U_\infty = 13.8m/s$ and of the nonlinear system in the right-side view.

Control effort is measured in voltage applied to the piezoelectric limited to a maximum of $200V$. This bounds the closed loop flutter speed for which the control effort required is higher then this maximum or has too much oscillation. Flutter onset for closed loop system is delayed up to $U_\infty = 16.5m/s$ for both linear and nonlinear model. These limits are for the controller with the worst performance and consider small perturbation on the initial conditions. No further adjustment of controller gains are attempted to increase this performance. For LQR method, flutter onset is increased up to $U_\infty = 17.6m/s$.

4. CONCLUDING REMARKS

An assessment of the aeroelastic behavior of a typical section was presented for a structural nonlinearity of hardening in pitch stiffness. Three different control strategies (eigenstructure assignment, LQR and fuzzy logic controller) were evaluated for the suppression of undesired vibration and postponement of the flutter boundary with piezoelectric actuation. The tested controllers stabilized the system for both linear and nonlinear response with an improvement of the predicted closed loop flutter speed of at least 24%.

Further experiments are planned to be soon performed in order to validate the results obtained computationally and to have a better assessment of the closed-loop system. Also an extension of the computational model to include uncertainties and other non-modelled nonlinearities is required to increase controllers robustness.

5. ACKNOWLEDGMENTS

The authors acknowledge the financial support of FAPESP (grant 2013/10117-2).

6. REFERENCES

Andry, A.N.J., Shapiro, E.Y. and Chung, J.C., 1983. "Eigenstructure assigment for linear systems". *IEEE*.

Bisphinghoff, R.L., Ashley, H. and Halfman, R.L., 1996. *Aeroelasticity*. Dover Publications.

Block, J.J. and Strganac, T.W., 1998. "Applied active control for a nonlinear aeroelastic structure". *Journal of Guidance, Control, and Dynamics*, Vol. 21, No. 6, pp. 838–845.

Chen, P., Sarhaddi, D. and Liu, D., 1998. "Limit-cycle-oscillation studies of a fighter with external stores." In *Proceedings of the 39th AIAA Structures, Structural Dynamics and Materials Conference*.

Denegri, C.M. and Johnson, M.R., 2001. "Limit cycle oscillation prediction using artificial neural networks". *Journal of Guidance, Control, and Dynamics*, Vol. 24, No. 5, pp. 887–895.

Dobbs, S., Miller, G. and Stevenson, J., 1985. "Self-induced oscillation wind tunnel test of a variable sweep wing". *AIAA Paper*, Vol. 85, pp. 86–92.

Dowell, E.H., Edwards, J. and Strganac, T.W., 2003. "Nonlinear aeroelasticity". *Journal of Aircraft*, Vol. 40, No. 5, pp. 857–874. doi:10.2514/2.6876.

Ehlers, S.M. and Weisshaar, T., 1993. "Static aeroelastic control of an adaptive lifting surface". *Journal of Aircraft*, Vol. 30, No. 4, pp. 534–540.

Fung, Y.C., 1993. *An Introduction to the Theory of Aeroelasticity*. Dover Publications, Inc, New York.

Hartwich, P.M., Dobbs, S.K., Arslan, A.E. and Kim, S.C., 2001. "Navier-stokes computations of limit-cycle oscillations for a b-1-like configuration". *Journal of aircraft*, Vol. 38, No. 2, pp. 239–247.

Heeg, J., 1993. "Analytical and experimental investigation of flutter suppresion by piezoeletric actuation". Technical report, NASA.

Jantzen, J., 1999. "Tuning of fuzzy pid controllers". Technical report, Technical University of Denmark.

Ko, J., Strganac, T.W. and Kurdila, A.J., 1999. "Adaptive feedback linearization for the control of a typical wing section with structural nonlinearity". *Nonlinear Dynamics*, Vol. 18, No. 3, pp. 289–301.

Lavretsky, E. and Wise, K.A., 2013. *Robust and Adaptative Control*. Springer.

Lee, B., Gong, L. and Wong, Y., 1997. "Analysis and computation of nonlinear dynamic response of a two-degree-of-freedom system and its application in aeroelasticity". *Journal of Fluids and Structures*, Vol. 11, No. 3, pp. 225–246.

Lee, B., Price, S. and Wong, Y., 1999. "Nonlinear aeroelastic analysis of airfoils: bifurcation and chaos". *Progress in Aerospace Sciences*, Vol. 35, No. 3, pp. 205 – 334. doi:http://dx.doi.org/10.1016/S0376-0421(98)00015-3.

Li, D., Guo, S. and Xiang, J., 2010. "Aeroelastic dynamic response and control of an airfoil section with control surface nonlinearities". *Journal of Sound and Vibration*, Vol. 329, No. 22, pp. 4756 – 4771.

Preumont, A., 2012. *Vibration control of active structures: an introduction*, Vol. 50. Springer Science & Business Media.

Robert, W. *et al.*, 1997. "Vertical tail buffeting alleviation using piezoelectric actuators-some results of the actively controlled response of buffet-affected tails (acrobat) program".

Sears, W.R., 1940. "Operational methods in the theory of airfoil in non-uniform motion". *Journal of the Franklin Institute*.

Sheta, F., Harrand, V.J., Thompson, D.E. and Strganac, T.W., 2002. "Computation and experimental investigation of limit cicle oscillations of nonlinear aeroelastic systems". *Journal of Aircraft*. doi:10.2514/2.2907.

Singh, S.N. and Yim, W., 2003. "State feedback control of an aeroelastic system with structural nonlinearity". *Aerospace Science and Technology*, Vol. 7, No. 1, pp. 23–31.

Stevens, B.L. and Lewis, F.L., 1992. *Aircraft Control and Simulation*. John Wiley & Sons.

Theodorsen, T., 1935. "General theory of aerodynamic instability and the mechanism of flutter". Technical Report 496, NACA Report 496.

Vasconcellos, R.M.G., 2012. *Characterization and Detection of the Nonlinearity associated to Freeplay in Aeroelastic Systems (in Portuguese)*. Ph.D. thesis, Engeneering School of São Carlos - USP.

Yager, R.R. and Filev, D.P., 1994. *Essentials of Fuzzy Modeling and Control*. John Wiley & Sons.

7. RESPONSIBILITY NOTICE